BALKANTRIB'O5
5th INTERNATIONAL CONFERENCE ON TRIBOLOGY
JUNE.15-18. 2005
Kragujevac, Serbia and Montenegro

COATING ELASTIC-PLASTIC PROPERTIES DETERMINED BY MEANS OF NANOINDENTATIONS AND FEM-SUPPORTED EVALUATION ALGORITHMS

K.-D. Bouzakis, N. Michailidis
Laboratory for Machine Tools and Manufacturing Engineering, Mechanical Engineering Department, Aristoteles University of Thessaloniki, GR-54124 Thessaloniki, Greece

Abstract

*The fast and fully automated software "FANOS" (**F**ast **A**pproach of stress-strain curves based on na**NO**indentation**S**) was applied to evaluate nanoindentation measurement results in order to determine stress-strain curves. Herein, laws describing the effect of the indentation load and depth on the developed stresses and strains are taken into account, deriving from the "SSCUBONI" ("**S**tress **S**train **CU**rves **B**ased **O**n **N**ano**I**ndentation") algorithm. In this way material's Young's modulus, yield strength and tangent moduli of plasticity can be defined.*
Characteristic results concerning various coatings elastic - plastic properties are introduced, obtained by means of the mentioned algorithms. A comparison was conducted between film Young's moduli determined by means of the previously mentioned algorithms and through existing analytical approximations of experimental nanoindentation results, demonstrating a sufficient convergence.

Keywords: *Nanoindentation, coatings, stress-strain curves, FEM simulation*

1. Introduction

Nanoindentation is a precise procedure to register continuously the course of the applied force versus the displacement (penetration depth). This measurement consists of two steps, the so-called loading stage and the unloading one. During the loading stage, an indentation load forces a diamond indenter to penetrate into the specimen. This load is gradually applied and at the same time the indentation depth is measured. When the load is fully removed, due to the resulting material plastic deformation, a remaining depth h_r occurs, depending on the material properties as well as on the applied load and the indenter geometry.

Elastic properties of hard materials can be determined by means of analytical evaluation procedures of nanoindentation results [1-4] and corresponding instruments of high accuracy have been developed [5]. The pointed out references have to be considered as indicative, since a large number of related ones are dealing with these issues. In recent publications the "SSCUBONI" algorithm for the continuous simulation of the nanoindentation was introduced, enabling the extraction of materials stress-strain elastic-plastic laws [6-8]. The accuracy of this algorithm has been proved to be high, however it is time consuming and demands experienced users. Based on the "SSCUBONI" algorithm the "FANOS" software was developed, allowing a faster evaluation of nanoindentation results in a working friendly interface, at the same high accuracy level [9].

In the present paper various coatings were investigated by means of these algorithms. The extracted mechanical properties results, as far as their elastic properties are concerned, were compared to the corresponding ones, which were determined by analytical approaches of nanoindentation results [1,4,5].

2. The continuous FEM supported simulation of the nanoindentation procedure by means of "SSCUBONI" and"FANOS" algorithms

A significant condition in nanoindentation evaluation procedures is the precise knowledge of the indenter tip geometry, since in nano-scale penetration depths, deviations from the ideal sharp tip geometry strongly affect the accuracy of the results [7,10]. A series of researchers deal with the determination of the actual indenter tip geometry [7,10-12] and manufacturers of nanohardness measurement instruments have established convenient calibration procedures [5,13]. These nano-deviations, which are due to indenter manufacturing accuracy limits, cannot be precisely described, even through Atomic Force Microscope (AFM) observations, according to which the tip geometry is not ideally sharp, but can be considered as a spherical one [11-13].

The indenter tip geometry of the applied Berkovich indenter, in the frame of the reslts introduced in the present paper, was approximated by means of nanoindentations on reference materials (Silicon (100): E= 182 GPa, HU= 6.9 GPa) and a FEM-based algorithm, introduced in [7] (see figure 1a). The actual tip axial section is considered to be described by a high order polynomial curve, which has a vertical tangent to the symmetry axis at the indenter tip (tangent 1) and a further one to the indenter side region (tangent 2). The radius of this curve at various positions versus the width of the indenter b, is presented in the diagram of figure 1a. The indenter tip region with form deviations is characterized by the indenter tip width b_h and the corresponding tip height t_h.

The continuous FEM simulation of the nanoindentation, due to accuracy reasons, is based on an axisymmetric FEM model of the semi-infinite material half space [7,14]. In this procedure the Berkovich or Vickers indenters are replaced by equivalent cones [7,8], as demonstrated in figure 1b. The associated boundary conditions and the finite elements discretisation network are explained in the details A and B respectively and the indenter

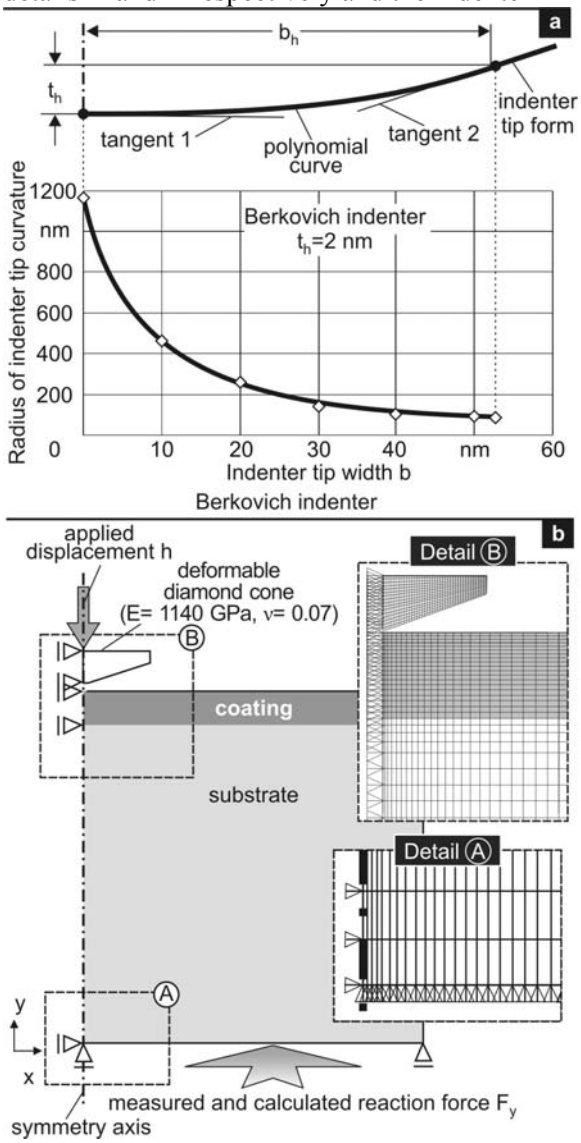

Figure 1: *a: Indenter tip form deviations. b: The FEM simulation model of the nanoindentation procedure.*

actual tip geometry is taken into account as described in figure 1a.

Based on the "SSCUBONI" algorithm [6-8] and considering the nanoindentation diagram of a tested material the related stress-strain curve can be determined. In the case of a 2 μm $(Ti_{46}Al_{54})N$ coating, the nanoindentation diagram is presented in the upper part of figure 2a. For the indentation depth h – indentation force F pairs, indicated as *I, II* and *III*, the von Mises equivalent stress and strain distributions within the coating in the contact region during nanoindentation are determined and illustrated

in the left and in the middle part of figure 2b respectively. Taking into account these stress

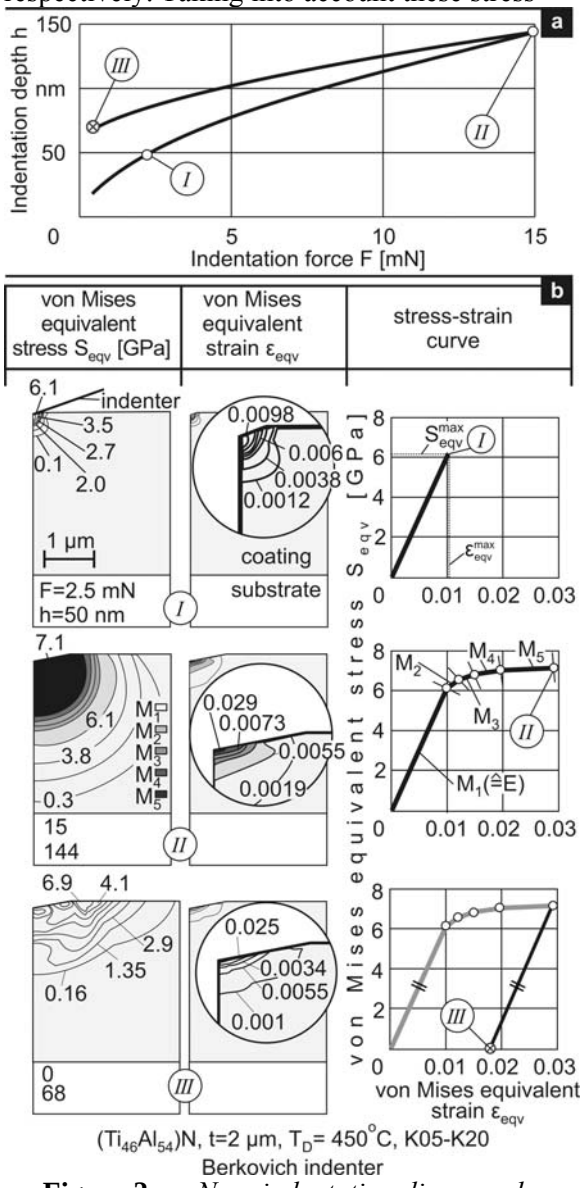

Figure 2: *a: Nanoindentation diagram. b: Stress and strain distributions for various indentation depths and stepwise determined stress-strain curve of a coating.*

and strain distributions, the stress-strain S_{max} - ε_{max} curve is stepwise determined, as shown in the right figure part. Up to a penetration depth of approximately 50 nm (*I*), the coating material is deformed almost elastically. The nanoindentation loading procedure terminates at a maximum penetration depth of 144 nm (*II*), when the maximum applied force of 15 mN is reached. In the corresponding stress-strain distribution graphs, the shadowed areas demonstrate that the material maximum deformation has entered progressively into the

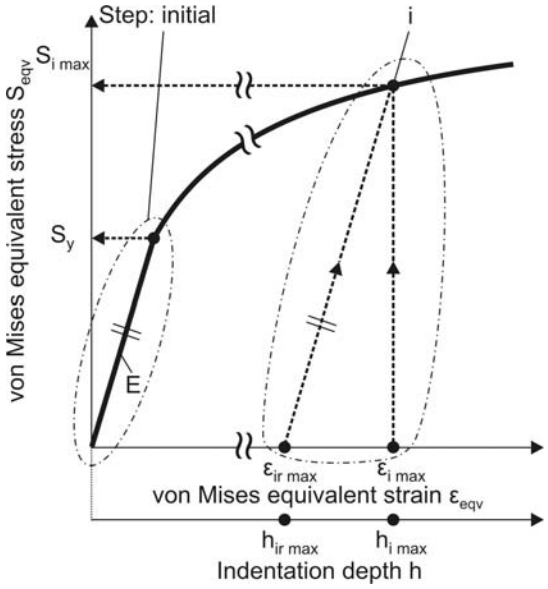

Figure 3: *Calculation steps in determining stress - strain curves by means of the applied "FANOS" software.*

regions of the stress-strain curve, indicated in the right figure part. The unloading stage reveals a remaining penetration depth of 68 nm as described in stage *III*.

The determination of elastic-plastic material laws takes place in individual calculation steps, by means of the applied algorithm "FANOS". Initially, considering successive h-F pairs extracted from the digitalized nanoindentation diagrams, the Young's modulus E and the yield strength S_y are defined (initial step, see figure 3). An algorithm based on extracted laws from the "SSCUBONI" method [6-8] gives the occurring maximum equivalent stress versus the indentation load and the occurring maximum equivalent strain versus the indentation depth [9].

In further calculation steps as for example in step i, the maximum equivalent stress $S_{i\,max}$ is determined as demonstrated in the same figure, considering the maximum indentation depth $h_{i\,max}$ and the remaining indentation depth $h_{ir\,max}$ corresponding to the strains $\varepsilon_{i\,max}$ and to the remaining strain $\varepsilon_{ir\,max}$ respectively. The intersection point of the line starting from the $\varepsilon_{ir\,max}$ point, parallel to the stress-strain curve in its elasticity region, with the vertical line at the strain $\varepsilon_{i\,max}$, reveals the maximum equivalent plastic stress $S_{i\,max}$ at the calculation stage i.

3. Application of "FANOS" software to determine coatings stress - strain curves

Figure 4 presents a view on the applied "FANOS" evaluation software. The presented screen is a first step, dealing with the nanoindentation diagram itself, where the h-F diagram is digitalized into a series of h-F pairs and the corresponding h-F diagram is plotted. The maximum indentation depth h_{max} and the maximum relaxation depth $h_{r\text{-}max}$ are determined as well.

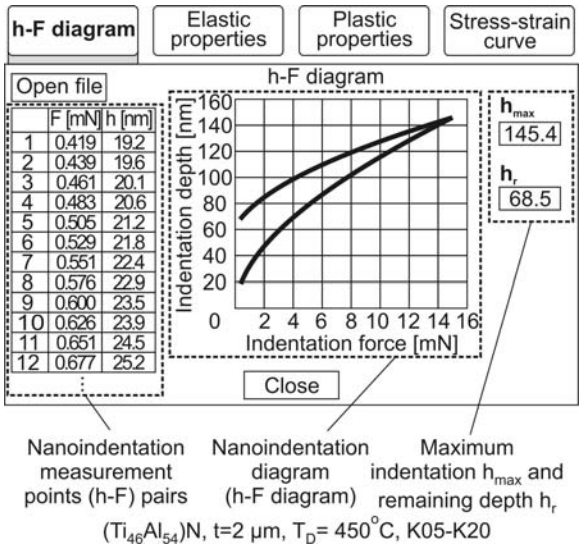

Figure 4: First calculation stage in the "FANOS software.

Assuming an Young's modulus E_{as}, the related maximum von Mises equivalent strain ε_{eqv} is determined by the "FANOS" algorithm. A new value of the Young's modulus, E_{cal} is then extracted. For a wide range of assumed Young's moduli E_{as}, the corresponding Young's moduli E_{cal} are calculated and the deviation of the assumed to the calculated ones $|\Delta E|=|E_{as}-E_{cal}|$ is registered, as shown in figure 5a. According to this plot and to the ones in figure 5b, only for the value of an assumed Young's modulus E_{as} equal to 610 GPa, i.e. equal to the determined one through [6-8], the related deviations are limited below 1% up to an indentation depth of 52 nm. This indentation depth corresponds to the material elastic deformation limit, i.e. to the yield strength S_y, which amounts approximately to 6.1 GPa. The deviations have a steep increase over this indentation depth.

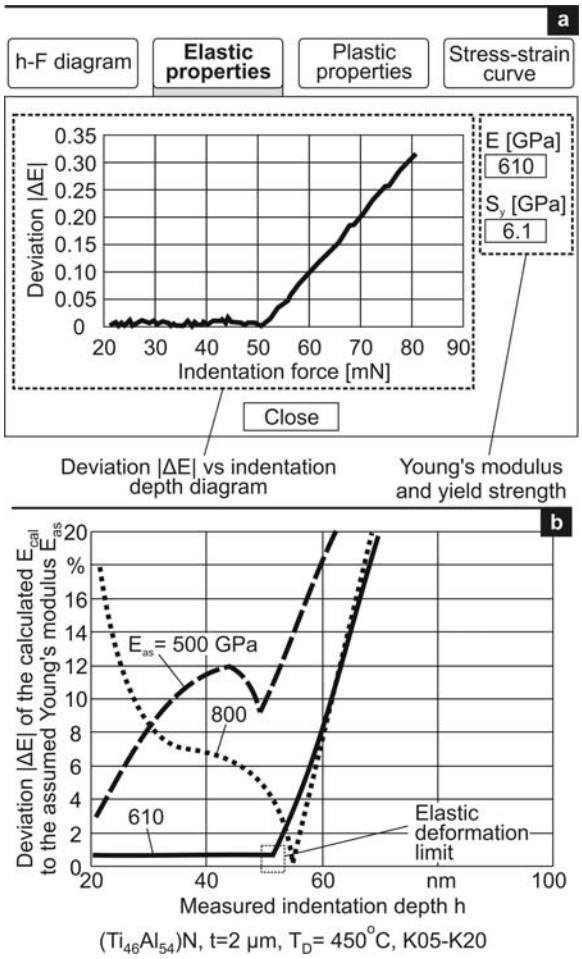

Figure 5: *a: Determination of coating Young's modulus and yield strength through "FANOS" software. b: Deviations |ΔE| versus the indentation depth, for various assumed Young's moduli.*

By conducting further nanoindentations at different indentation loads i.e. different maximum indentation depths it is possible to determine by the "FANOS" algorithm further stress-strain pairs ($S_{i\ max}$ - $\varepsilon_{i\ max}$) in the material plasticity area, according to the procedure of figure 3, thus constructing in a stepwise way a complete stress-strain curve. In the case of $(Ti_{46}Al_{54})N$ coating, nanoindentations at 3 up to 15 mN were conducted and the corresponding results are presented in the diagrams in the left part of figure 6. By means of h-F value pairs following an ascending order of indentation loads, Young's modulus and yield strength in the initial calculation stage are determined as well as the point (0') of the stress-strain curve, corresponding to the elastic region limit.

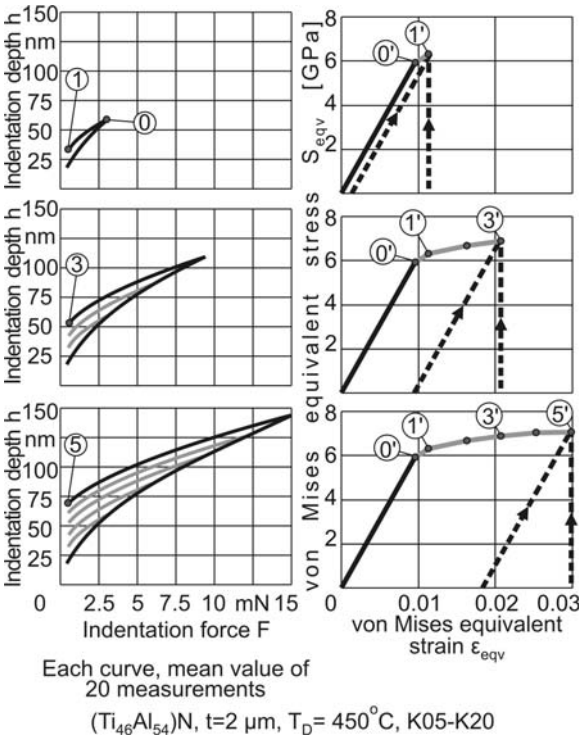

Figure 6: *Typical example of a stress-strain curve determination by means of the "FANOS" software.*

Moreover, the points (1') to (5') of the stress-strain curve in the plastic deformation region are stepwise obtained from further calculations.
In a final stage of the applied "FANOS" software, the stress-strain curve points in the material plasticity region are determined, taking into account the extracted h_{max} and $h_{r\text{-}max}$ values, as well as the Young's modulus defined in a previous calculation stage (see figure 7a). "FANOS" software terminates with the graphical presentation of the determined stress-strain curve (see figure 7b). Comparing the Young's modulus calculated by means of the "FANOS" algorithm to the corresponding one obtained with the "SSCUBONI" algorithm, i.e. 610 and 620 GPa respectively (see figure 7c), it is evident that there is a good agreement between these two methods. On the other hand, the Young's modulus determined by means of the analytical method [1,4,5] amounts to 494 GPa. The corresponding deviations from the "FANOS" results are in all cases less than 19%.

FANOS algorithm was further applied to determine the constitutive laws of various coatings. Hereupon nanoindentations at various indentation loads (3 up to 15 mN) were

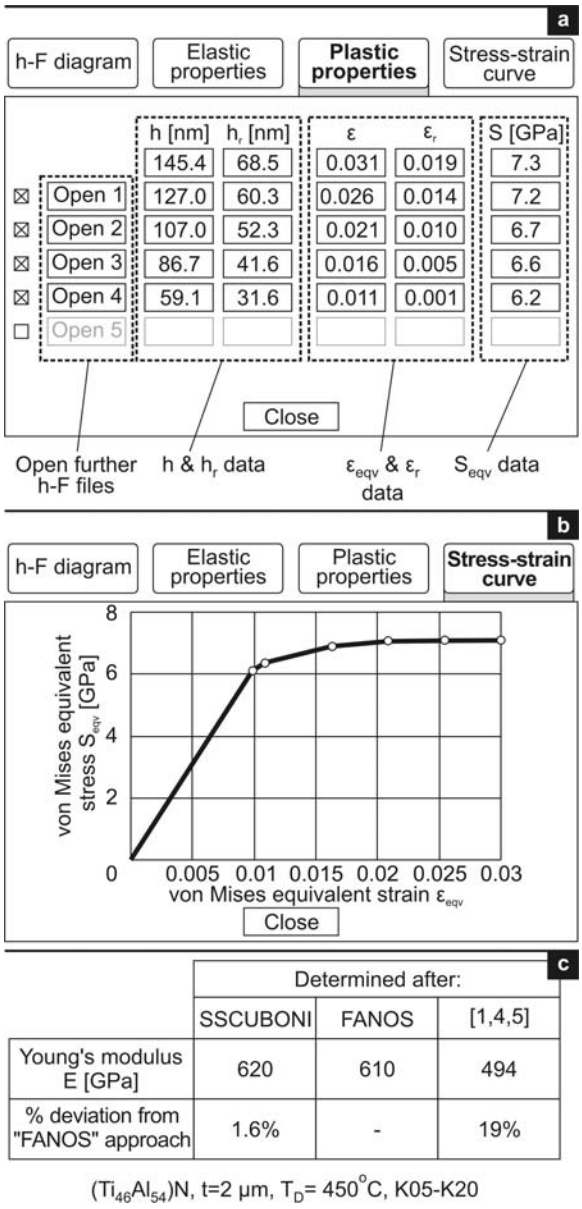

Figure 7: *a: Stress and strain pairs determined through the "FANOS" software. b: Coating stress-strain curve calculated by means of the "FANOS software. c: Deviations of the calculated coating Young's modulus according to various methods.*

conducted. The corresponding results for the $(Ti_{35}Al_{65})N$ coating [15] are presented in the upper part of figure 8. Considering the h-F value pairs, the coating Young's modulus, its yield strength as well as its plastic properties are determined by means of both the "SSCUBONI" and "FANOS" algorithms. The related results agree well, as shown in the bottom part of the same figure, demonstrating an adequate

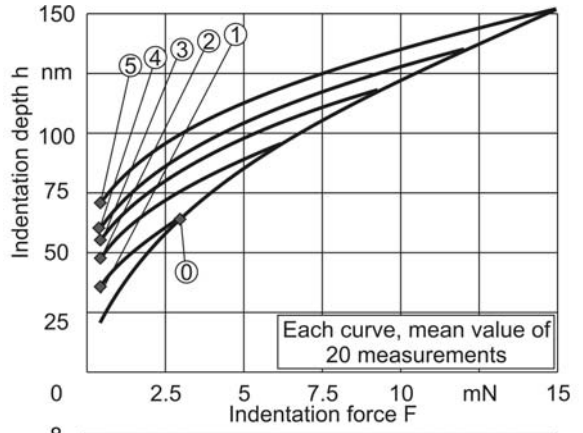

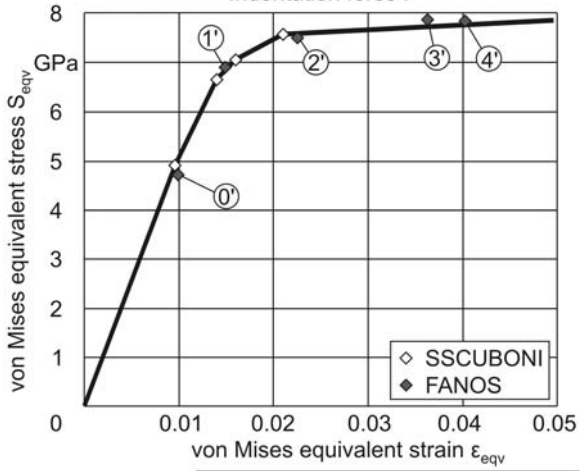

	Determined after:		
	SSCUBONI	FANOS	[1,4,5]
Young's modulus E [GPa]	510	500	490
% deviation from "FANOS" approach	2%	-	2%

$(Ti_{35}Al_{65})N$, t=3.5 μm, T_D= 475°C, K05-K20

Figure 8: *Nanoindentations at various indentation loads and comparison of the stress-strain pairs, determined for $(Ti_{35}Al_{65})N$ coating by means of various methods.*

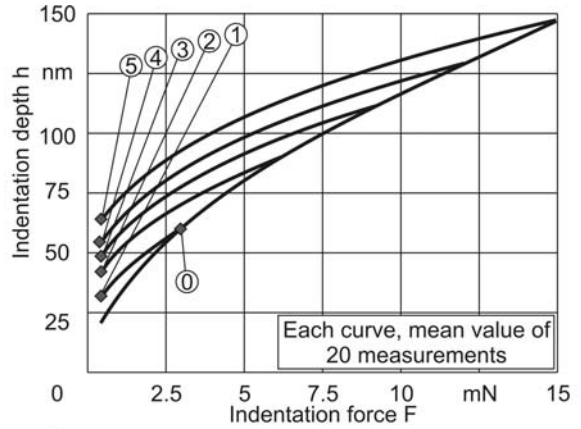

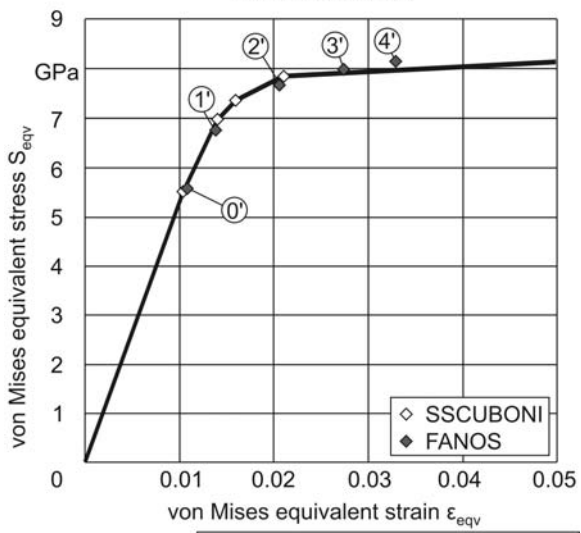

	Determined after:		
	SSCUBONI	FANOS	[1,4,5]
Young's modulus E [GPa]	530	525	460
% deviation from "FANOS" approach	1%	-	14%

CrAlN, t=3 μm, T_D= 450°C, K05-K20

Figure 9: *Nanoindentations at various indentation loads and comparison of the stress-strain pairs determined for CrAlN coating through various methods.*

convergence, with the deviation being less than 2%. In this case, the Young's modulus determined after [1,4,5] is close to the previously mentioned values, with the corresponding deviation from the "FANOS" algorithm value, also less than 2%.

Further nanoindentations were conducted on a CrAlN coating and the results extracted are shown in the upper part of figure 9. The stress – strain curves determined through the "SSCUBONI" and "FANOS" algorithms are practically the same, which verifies again the good agreement between the applied algorithms in determining materials' constitutive laws. A comparison of the Young's modulus calculated after "SSCUBONI", "FANOS" and [1,4,5] procedures shows again a good agreement between the obtained results, with deviations relatively to "FANOS" less than 14%.

4. Conclusions

The "FANOS" software was developed, based on results obtained with the aid of the "SSCUBONI" algorithm. "FANOS" allows a

fast and accurate evaluation of nanoindentation results, by means of a working friendly interface. The previously mentioned algorithms were applied to determine coatings elastic-plastic properties and a comparison between extracted results, in three coating cases was conducted. Both computational procedures share almost the same results, as far as material stress-strain curves are concerned. Comparing these results to the calculated ones by means of widely used analytical approximations of experimental nanoindentation results after [1,4,5], the Young's modulus showed relatively low deviations. In this way the "FANOS" software is proved to be an efficient tool for the determination of coatings stress-strain curves based on nanoindentations.

5. References

[1] W.C. Oliver, and G.M. Pharr, J. Mater. Res. 7:1564-1583 (1992).

[2] J. Alcala, A. E. Giannakopoulos, and S. Suresh, J. Mater. Res. 13:1390-1400 (1998).

[3] T. Chudoba, N. Schwarzer, and F. Richter, Surf. and Coat. Technol. 127:9-17 (2000).

[4] ISO 14577, Metallic materials - Instrumented indentation test for hardness and materials parameters, 2002.

[5] HELMUT FISCHER GmbH +Co Evaluation Manual of Indentation Procedure, Sindelfingen - Germany, (2000).

[6] K.-D. Bouzakis, N. Michailidis, and G. Erkens, Surf. and Coat. Technol. 142/144:102-109 (2001).

[7] K.-D. Bouzakis, N. Michailidis, S. Hadjiyiannis, G. Skordaris, and G. Erkens, Zeitschrift fuer Metallkunde, 93:862-869 (2002).

[8] K.-D. Bouzakis, N. Michailidis, S. Hadjiyiannis, G. Skordaris, and G. Erkens, Journal of Materials Characterisation, 49:149-156 (2003).

[9] K.-D. Bouzakis, and N. Michailidis, A fast and accurate approach to determine materials' stress-strain curves based on nanoindentations and corresponding FEM simulations, Proceedings of 6th MESOMECHANICS conference, 31 May – 4 June 2004, Patras Greece, pp. 69-78.

[10] K. Herrmann, N.M. Jennett, W. Wegener, J. Meneve, K. Hasche, and R. Seemann, Thin Solid Films, 377/378:394-400 (2000).

[11] N.M. Jennett, and J. Meneve, Proc. MRS Symp. 522:239-244 (1998).

[12] N.M. Jennett, G. Shafirstein, and S.R.J. Saunders, VDI Berichte 1194, VDI-Verlag GmbH, Dusseldorf, pp. 201-210 (1995).

[13] B. Bhushan, and B.K. Gupta, Macro and Micromechanical and Tribological Properties, in Handbook of hard coatings - Deposition Technologies-Properties and Applications, ed., R. F. Bunshah, Noyes Publications - Park Ridge - New Jersey - USA, pp. 229-369 (2001).

[14] Swanson Analysis System, INC., ANSYS user manuals, Vol.1 Theory, Vol.2 Procedures, Vol.3 Elements, Vol.4 Commands, (1995).

[15] G. Erkens, R. Cremer, T. Hamoudi, K. -D. Bouzakis, I. Mirisidis, S. Hadjiyiannis, G. Skordaris, A. Asimakopoulos, S. Kombogiannis, J. Anastopoulos and K. Efstathiou, Surface and Coatings Technology, Surf. and Coat. Technol. 177/178: 727-734 (2004).